Energy Conversion and Management 315 (2024) 118748

Contents lists available at ScienceDirect

Energy Conversion and Management

journal homepage: www.elsevier.com/locate/enconman

Reformer + Membrane separator plant for decarbonized hydrogen production from Biogas/Biomethane: An experimental study combined to energy efficiency and exergy analyses

Henry Bryan Trujillo Ruales [a], Alex Spadafora [a,b], Piergiuseppe Fiore [a], Jan Veres [c], Alessio Caravella [b], Adolfo Iulianelli [a,*]

[a] National Research Council (CNR) of Italy, Institute on Membrane Technology (CNR-ITM), via P. Bucci 17C, Rende (CS), 87036, Italy
[b] DIMES Dpt. of University of Calabria, Via P. Bucci 34/B, Rende (CS), 87036, Italy
[c] Technical University of Ostrava, Energy and Environmental Technology Centre, Energy Research Centre, 17. listopadu 2172/15, 708 00 Ostrava-Poruba, Czech Republic

ARTICLE INFO

Keywords:
Decarbonized hydrogen
Membrane engineering
Exergy
Energy efficiency
Steam reforming of biogas/biomethane

ABSTRACT

Nowadays, the world energy production is still based on the exploitation of fossil fuels, mainly oil, coal, and natural gas, responsible for large greenhouse emissions in the environment. According to the measures proposed by the European Green Deal to meet the carbon neutrality by 2050, the decarbonisation of the ~~global~~ energy production processes represents a top priority. Hydrogen represents a carbon-free energy carrier, useful to drive the society toward a decarbonized-economy. The novelty of this work is represented by the experimental generation of clean hydrogen by a two stages plant constituted of a biogas/biomethane steam reformer and a Pd-Ag membrane separator, meanwhile applying on this simple case the methodology of the exergy analysis, identifying the main losses and suggesting improvements. Hence, it deals with the exergy analysis of the whole system with the process intensification operated by the membrane separator adopted instead of using several stages to separate/purify hydrogen – as conventionally done after the reforming stage (two water gas shift reactors, high and low temperature, followed by a pressure swing adsorption stage) – with the objective of recovering decarbonized hydrogen coming from the biogas/biomethane steam reformer, meeting the European targets indicated by the Clean Hydrogen Alliance. This approach allowed to understand the amount of irreversibilities present in such a system as well as how the thermal efficiency may be influenced by a number of parameters, constituting globally a baseline for the scaling up of this process technology from lab to bench/pilot scale. The best results of this work highlight that the utilization of biomethane in the feed stream to generate hydrogen resulted to be a better choice than biogas in terms of thermal efficiency (based on the lower heating value) of the whole system, equal to 73 % at 773 K, while the highest percentage of exergy destruction was concentrated in the condensation stage, with values varying between 76 % and 93 %, depending on the feed stream typology. The two stages system was able to meet the "decarbonized hydrogen production target 2027", with a hydrogen recovery of 90 % and a purity of 99.9999 %. Last but not least, the overall exergy destroyed efficiency of the overall system in the two analyzed cases was 92 % (biomethane feed stream) and 88 % (biogas feed stream), respectively.

1. Introduction

At present, the World is facing with an increase in energy consumption that is growing steadily due to factors such as the development in the transportation and industry areas as well as the improvement of the form of life of the human beings [1]. Still, different human activities represent relevant contributors to climate change, as a consequence of the increase of greenhouse gases (GHGs) emissions and the environmental pollution as well [2]. During COP21, several Countries adopted the so-called Paris Agreement to contrast the climate change, limiting the pollutants emission to stop the Earth's temperature increase to 2 K maximum [3].

Today, most of the world energy production comes from derived of

* Corresponding author.
E-mail addresses: a.iulianelli@itm.cnr.it, adolfo.iulianelli@cnr.it (A. Iulianelli).

https://doi.org/10.1016/j.enconman.2024.118748
Received 12 April 2024; Received in revised form 27 June 2024; Accepted 27 June 2024
Available online 1 July 2024

Nomenclature

Ch_{4-in}	Inlet methane molar flow rates (mol/s)
Ch_{4-out}	Outlet methane molar flow rates (mol/s)
$\dot{E}in$	Inlet exergy destruction (W)
$\dot{E}out$	Outlet exergy destruction (W)
$\dot{E}X_i^W$	Exergy flows related to work (W)
$\dot{E}X_i^Q$	Exergy flows related to heat exchange (W)
$\dot{E}X_i^{\dot{M}_{In}}$	Exergy flow related to the inlet streams (W)
$\dot{E}X_i^{\dot{M}_{Out}}$	Exergy flow related to the outlet streams (W)
$\dot{E}X_d$	Destruction exergy (W)
$H_{2-permeate}$	Hydrogen molar flow rates in the permeate side (mol/s)
$H_{2-retentate}$	Hydrogen molar flow rates in retentate side (mol/s)
hi	Values of enthalpy of the species i (KJ $kmol^{-1}$)
hi_o	Values of enthalpy of the species i in the reference state (KJ $kmol^{-1}$)
J_{h2}	Hydrogen permeating flux (mol m^{-2} s^{-1})
P_o	Reference pressure (Pa)
Ti	Temperature of the external source (K)
T_o	Reference temperature (K)
$Q_{permeate}$	Total molar flow rate of the permeate stream (mol/s)
Q_i	Net heat through a system (W)
Si	Values specific entropy of the species i (KJ $kmol^{-1}$ K^{-1})
Si_o	Values specific entropy of the species i in the reference state (KJ $kmol^{-1}$ K^{-1})
R	Ideal gas constant (KJ $kmol^{-1}$ K^{-1})
W	Work that is potentially recoverable by the system (W)
Wrev	Effective work through reversible processes (W)

List of greek letters

Δp_{h2}	Hydrogen partial pressure difference between retentate and permeate sides (Pa)
α	Selectivity (−)
τ_i	Carnot factor (−)
Ψ_{ph}	Physical exergy (W)
Ψ_{ch}	Chemical exergy (W)
η_{ex}	Exergy efficiency (−)
η_{H2}	Thermal efficiency (−)

List of subscripts

BSR	Biogas steam reforming
CD	Cryogenic distillation
GC	Gas chromatograph
GHGs	greenhouse gases
LHV	Lower heating value
MS	Membrane separation
MFCs	Mass flow controllers
PSA	Pressure swing adsorption
S/C	Steam-carbon ratio
TR	Fixed bed reactor

fossil fuels such as oil, coal, and natural gas, which are responsible for huge emissions of GHGs, leading to a rise in the average temperature of the planet. Hydrogen is considered as the new, alternative, and environmentally friendly energy carrier, constituting an essential alternative to substitute the fossil sources dependence, and main subject to lead to the "Hydrogen economy" [4].

Currently, there are different sources for producing hydrogen: natural gas, derived of biomass, light hydrocarbons, carbon, nuclear power plants and electrolysis. Industrially, most of the global hydrogen output comes from the steam reforming of natural gas, and it is called "grey hydrogen", responsible for abundant CO_2 emissions in the atmosphere [5]. In the last few years, particular attention has been paid on the production of hydrogen from renewable biological sources such as biogas, wood, or ethanol [6–9]. In particular, biogas is a renewable source and represents an ideal candidate to substitute natural gas in the production of hydrogen by steam reforming reaction [10]. It is derived from biomass and may be produced, for example, by anaerobic fermentation of different organic, agro-industrial, and anthropogenic residues, contributing to promote the objectives of the Circular Economy [11,12].

Among the different technologies for converting biogas into hydrogen, there are catalytic reactions such as steam and dry reforming, combined steam and dry reforming of CO_2, auto thermal reforming and partial oxidation as well [11–15]. The fundamental process for hydrogen production from biogas/biomethane may be represented by a complex reaction system as reported below:

Steam reforming of methane.

$$CH_4 + H_2O \rightarrow CO + 3H_2 \Delta H = 206.1\ kJ/mol \quad (1)$$

Water gas shift reaction

$$CO + H_2O \rightarrow CO_2 + H_2 \Delta H = -41.2\ kJ/mol \quad (2)$$

Reverse methanation reaction

$$CH_4 + 2H_2O \rightarrow CO_2 + 4H_2 \Delta H = 164.9\ kJ/mol \quad (3)$$

Dry reforming of methane.

$$CH_4 + CO_2 \rightarrow 2CO + 2H_2 \Delta H = 247.3\ kJ/mol \quad (4)$$

Decomposition of methane.

$$CH_4 \rightarrow C + 2H_2 \Delta H = 74.9\ kJ/mol \quad (5)$$

Carbon monoxide reduction

$$CO + H_2 \rightarrow C + H_2O \Delta H = -131.3\ kJ/mol \quad (6)$$

Boudouard reaction

$$2CO \rightarrow C + CO_2 \Delta H = -172.4\ kJ/mol \quad (7)$$

Carbon dioxide reduction

$$CO_2 + 2H_2 \rightarrow C + 2H_2O \Delta H = -90.1\ kJ/mol \quad (8)$$

Conventionally, this complex reaction system takes place in a temperature range between 973 and 1173 K. The products obtained from biogas steam reforming (BSR) reaction are a hydrogen-rich gaseous mixture, containing also unconverted CH_4, CO_2, CO and steam [14,15]. To produce the so-called blue hydrogen (high grade hydrogen combined to the total CO_2 capture), useful in industry and in various energy systems, hydrogen separation/purification plays a relevant role. Pressure swing adsorption (PSA) and cryogenic distillation (CD) are currently the most adopted conventional processes for hydrogen purification [16,17]. Nevertheless, they show several drawbacks as they are expensive, energy-demanding, and envelope the use of large-scale plants. In addition to the aforementioned processes, membrane separation (MS) has become an attractive option pursuing the principles of the Process Intensification Strategy [18,19]. Among the main features that this technology presents, lower energy consumption and operating costs, continuous, flexible and environmentally friendly operations, and reduced plant size, are the characteristics guaranteed by the membrane engineering applied to hydrogen separation and purification [20].

Selective membranes for separating hydrogen may be manufactured according to various materials typologies, such as polymeric [19,20],

porous and non-porous inorganic [21–27]. The dominant membrane material for high grade hydrogen separation is represented by palladium and its alloys [18,22]. In particular, Pd-alloys possess the ability of dissociating and dissolving hydrogen [28], presenting good thermal and mechanical stability [29], increased resistance to surface poisoning [5] and high hydrogen perm-selectivity with respect to all of the other gases [6,30].

Regarding to the hydrogen production, worth of investigation is the analysis of this process from an energy conservation point of view, useful to evaluate if it is able to save energy and, in the meantime, to reduce the overall energy costs [31–35]. Indeed, thermodynamic studies consider the energy contribution in terms of energy conservation only, which alone is insufficient as it does not consider the irreversible nature of the involved processes due to their entropic nature [36]. Therefore, the performance improvement of every energy process requires the reduction of these irreversibilities [37]. In this regard, exergy is defined as the maximum reversible work that can be obtained bringing a system in equilibrium with its environment. Since exergy is destroyed any time an irreversible process takes place, the exergy analysis may be employed to identify the process unit in which the most significant losses in energy quality take place [34–36]. On one hand, the calculation of the energy efficiency indicates the amount of energy stored in a system; on the other hand, the exergy efficiency indicates the convertibility of that energy into useful work [38].

In this study, a fully hydrogen perm-selective self-supported Pd-Ag membrane separator is adopted instead of the conventional high and low temperature water gas shift reactors followed by a PSA unit to purify a hydrogen rich stream coming out from a fixed bed reformer, in which the steam reforming of synthetic biogas or biomethane streams are carried out. In this regard, evaluating if the two stages plant better perform starting from using biogas instead of biomethane to meet the strict European targets contained in the Strategic Research and Innovation Agenda 2024–2030 set by the EU Clean Hydrogen Agency [38] is of high interest as biogas utilization would allow of avoiding a pretreatment stage to obtain biomethane, with advantages in terms of energy and cost saving. A few works are present in the open literature about the energy and exergy analyses involving membrane technology, but all of them focus on membrane reactors [37,39–41] or on conventional reformers used to generate hydrogen from different sources [42]. Even though this work deals with a specific-case study in which a number of variables (membrane area, space velocity, sweeg gas flow rate) affecting the whole hydrogen production/purification process have been excluded by the investigation, the novelty is represented by the analysis from both 1st and 2nd principles of thermodynamics, which integrates energy and entropy balances in an overall exergy evaluation, carried out on a two stages system constituted of a fixed bed reactor and a Pd-Ag membrane separator. In particular, the energy efficiency and exergy analyses have been carried out on the former and on the ancillary (boiler, mixer, condenser) devices to evaluate the percentage distribution of the irreversibilities present in the proposed two stages system. Hence, the energy and exergy analyses, coupled to the robust experimental campaign proposed in this work, may constitute an important contribution in the scaling up of this process technology from lab to bench/pilot dimension. To the best of our knowledge, no studies focus on the aforementioned approach and the latter may constitute a first contribution in this field.

2. Experimental

2.1. Reformer + membrane separator system

The schematic of the two stages integrated system of this work is shown in Fig. 1. In the first stage, a conventional tubular fixed bed reactor (TR) (15 cm in length and 1 cm of outer diameter) is adopted to carry out the steam reforming of synthetic biogas or biomethane over a Ni-based catalyst, Fig. 2a.

A hydrogen-rich stream (TR reformate) coming out from the TR is fed to the second stage process of the overall system, in which a hydrogen membrane separator (Fig. 2B) houses a self-supported Pd-Ag membrane (Fig. 2C), which allows the hydrogen separation/purification. The decarbonized hydrogen stream is collected in the permeate stream of Stage II, whereas the retentate represents the stream unpermeated through the Pd-Ag membrane.

According to the schematic of the entire flow-sheet (Fig. 1) (including the TR and the auxiliary devices) of Stage I, the steam reforming reaction takes place in the TR, which is packed with 3 g of a Ni-based catalyst.

The TR is housed in an electric furnace and the synthetic biogas and biomethane streams and hydrogen (the latter to reduce the catalyst) are fed to the TR via dedicated pipelines, connected to pure gas cylinders (CO_2, CO, CH_4, H_2) and a mixer, by Brooks Instruments mass flow controllers (MFCs), controlled by a MFCs station with a dedicated Excel macro, operated by Lira (Italy) software. Deionized water is delivered through an HPLC model P680 DIONEX pump, which is preheated (vaporized) and mixed with the synthetic biogas/biomethane streams, respectively, before entering the TR. A cold trap containing a condenser immersed in an ice bath is placed on the reformate stream coming out from the TR in order to condensate the steam and supply the hydrogen-

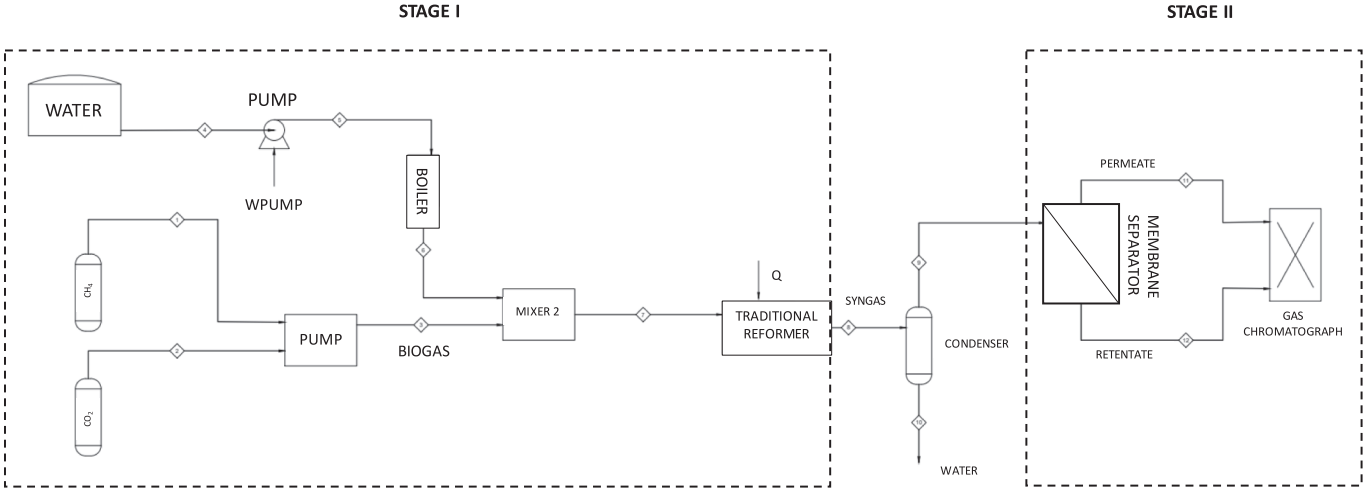

Fig. 1. Schematic of the two stages system for decarbonized hydrogen generation by biogas/biomethane steam reforming. Stage I: traditional reformer; Stage II: Pd-Ag membrane separator.

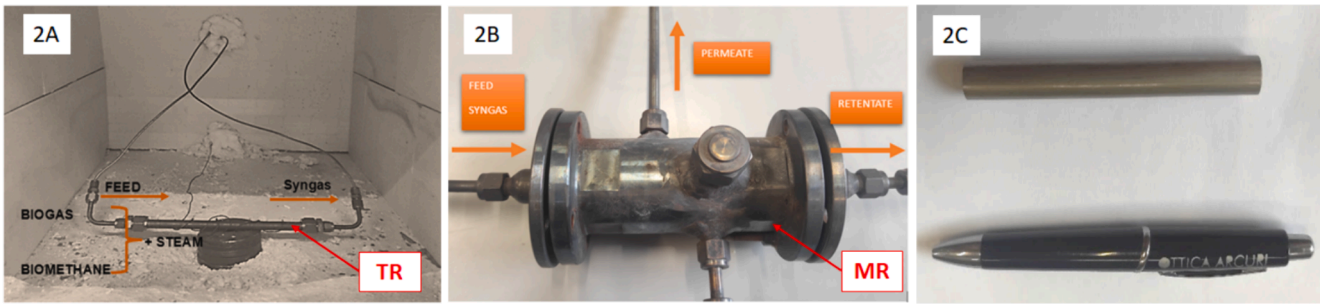

Fig. 2. A) traditional reformer; B) Pd-Ag membrane separator; C) dense self-supported Pd-Ag membrane.

rich stream to the membrane separator under dry conditions.

Stage II consists of a tubular stainless-steel membrane separator module (Fig. 2B), with a length of 14 cm and an internal diameter of 2 cm, housing a tubular, dense, self-supported Pd-Ag membrane (Fig. 2C), showing a length of 10 cm, an outer diameter of 1.0 cm, and a thickness of 150 μm. The Pd-Ag membrane is blocked to the MS flange by two carbon gaskets useful to prevent the permeate and retentate streams mixing. Fig. 1 illustrates also the schematic of the MS, where the permeate stream collects the decarbonized hydrogen, whereas the retentate stream contains the unpermeated gases through the Pd-Ag membrane.

An inert sweep gas (N_2) is flowed in the permeate side of the MS in order to favor the hydrogen permeation driving force across the membrane, decreasing as much as possible the hydrogen partial pressure in the permeate side. Nevertheless, N_2 has been adopted as sweep gas for easy lab-scale operations, but under real operations it may be substituted by steam in order to recover pure hydrogen in the permeate side for condensation of the steam. Both permeate and retentate streams are hence analyzed by GC.

2.2. Experimental details and performance parameters

3 g of a Ni-based catalyst has been packed inside the TR. It has been produced by combustion method and, before starting the reaction tests, it has been reduced by flowing pure hydrogen (15 mL/min) for 2 h at 873 K and atmospheric pressure.

Being out of the scopes of this work to analyze the effect of byproducts (<1%vol) present in both real biogas and biomethane streams, we adopted a synthetic biogas mixture fed to the TR, constituted of CH_4 and CO_2 with molar compositions equal to 60/40 (according to most of the biogas compositions obtained by anaerobic digestion [10]),as well as a synthetic biomethane stream equal to 98/2 (respecting the maximum limit of 2 %vol of CO_2 permitted in biomethane streams as indicated by the International Energy Agency). Experimental catalytic tests have been carried out in the TR at 873 K and 1 bar, varying the H_2O/CH_4 feed molar ratio (S/C) from 2/1 to 4/1. The feed stream compositions based on both synthetic biogas and biomethane mixtures are reported in Table 1 and Table 2 as a function of the S/C ratio.

The MS has been heated up to 673 K flowing N_2 as an inert gas. Single gas permeation tests (H_2 and N_2) have been carried out to establish the reference ideal H_2/N_2 perm-selectivity ($\alpha_{H2/N2}$), and the hydrogen permeating flux (J_{H2}) through the membrane has been measured as a function of the hydrogen permeation driving force across the membrane, expressed in terms of hydrogen partial pressure difference between retentate and permeate sides (Δp_{H2}).

Table 1
Feed compositions (based on the synthetic biogas mixture) as a function of S/C feed ratio.

S/C [-]	x_{CH4} [% mol.]	x_{CO2}[% mol.]	X_{H2O}[% mol.]
2	27.3	18.2	54.5
3	21.4	14.3	64.3
4	17.6	11.8	70.6

Table 2
Feed compositions (based on the synthetic biomethane mixture) as a function of S/C feed ratio.

S/C [-]	x_{CH4} [% mol.]	x_{CO2}[% mol.]	X_{H2O}[% mol.]
2	33.1	0.6	66.3
3	24.8	0.5	74.7
4	19.9	0.4	79.7

A HP model type 6890 Series GC System has been used to analyze all the TR and MS outlet gas compositions. It is equipped with three packed columns: Porapack R 50/80 (8 ft 1/8 in) in series with a Carboxen, 1000 (15 ft 1/8 in), and a molecular sieve 5 °A (6 ft 1/8 in), using Ar as the carrier gas. The GC is controlled by a software useful to calculate the streams compositions by the Standard Gas Method procedure (He is used as Standard Gas, 25 mL/min).

Process parameters studied in this work to analyze the performance of the TR and MS include: methane conversion, hydrogen yield, hydrogen recovery and purity. They are reported below:

$$\text{Conversion of } CH_4\,(\%) = \frac{CH_{4-IN} - CH_{4-OUT}}{CH_{4-IN}} \cdot 100 \tag{9}$$

where CH_{4-IN} and CH_{4-OUT} are the inlet and oulet methane molar flow rates, respectively.

$$H_2 \text{ yield}\,(\%) = \frac{H_{2-out}}{4{*}CH_{4-IN}} \tag{10}$$

where $4{\cdot}CH_{4-IN} = n_{H2,max}$ represents the maximum theoretical hydrogen producible by steam reforming of methane (1).

$$H_2 \text{ recovery}\,(\%) = \frac{H_{2-permeate}}{H_{2-permeate} + H_{2-retentate}} \cdot 100 \tag{11}$$

where $H_{2-permeate}$ and $H_{2-retentate}$ represent the hydrogen molar flow rates in the permeate and retentate sides of the MS, respectively.

$$H_2 \text{ permeate purity}\,(\%) = \frac{H_{2-permeate}}{Q_{permeate}} \cdot 100 \tag{12}$$

where $Q_{permeate}$ indicates the total molar flow rate of the permeate stream in the MS.

3. Methodology

The overall exergy performance analysis of the two-stages system (reformer and membrane separator) allows to assess the efficiency of the different stages involved in the decarbonized hydrogen production, making possible the identification of any critical point of the overall system and optimizing the whole process performance. According to the

definition of exergy [44], also reported previously, it is possible to define the following statement:

- Reference environment: it refers to the part of the environment surrounding the system in which the various intensive properties are unaffected by any process involving the equipment and its immediate surroundings. Therefore, the reference environment is considered free of irreversibility and uniform in terms of pressure (P_o = 1 bar and T_o = 298 K) [44].
- Dead state: this is considered when a system is in a different state to the environmental condition, which allows work to be developed. During the dead state, the environment and the system possess energy, but the exergy is equal to zero [43,44].
- Steady-state: under steady-state conditions, the total energy of a system is constant and when the change of this energy in the system is equal to zero. Therefore, the amount of energy entering a control volume (heat, mass, and work) must be equal to the amount of energy leaving the system. The energy balance can be defined as in the following equation [44]:

$$\dot{E}in - \dot{E}out = \frac{d\dot{E}syst}{dt} = 0 \tag{13}$$

Exergy balance directly derives from the coupling of energy and entropy balances [44]

$$\frac{d\dot{E}_x}{dt} = \sum_i \dot{E}x_i^{W} + \sum_i \dot{E}x_i^{Q} + \sum_i \dot{E}x_i^{\dot{m}_{in}} - \sum_i \dot{E}x_i^{\dot{m}_{out}} + \dot{E}x_d \tag{14}$$

$\dot{E}x_i^{W}$ and $\dot{E}x_i^{Q}$ are the exergy flows related to work and heat exchange with the environment. $\dot{E}x_i^{\dot{m}_{in}}$ and $\dot{E}x_i^{\dot{m}_{out}}$ are the exergy flows related to the inlet and oulet streams, $\dot{E}x_d$ the destruction exergy.

- Exergy associated to work: the analogy between work-related energy and exergy can be defined as follows [45]:

$$\sum_i \dot{E}x_i^{W} = \sum_i \dot{W}_i \tag{15}$$

- Exergy associated to heat: the heat transfer at a specific temperature is calculated as [44,46]:

$$\sum_i \dot{E}x_i^{Q} = \sum_i \dot{Q}_i \tau_i \tag{16}$$

where τ_i is called Carnot factor, which is related to the heat exchange between the system and the external source [44,46]:

$$\tau_i = \left(1 - \frac{To}{Ti}\right) \tag{17}$$

where To is the reference temperature, Ti the temperature of the external source and Q_i net heat through a system; it is positive when it enters the system and negative when it leaves the system.

- Exergy associated to mass flow: The exergy analysis consists of 4 different contributions: physical, chemical, potential and kinetics exergies [45,47,48]:

$$\sum_i \dot{E}x_i^{\dot{m}} = \sum_i \dot{m}_i \left(\psi_{ph} + \psi_{ch} + \psi_{pot} + \psi_{kin}\right) \tag{18}$$

- Physical exergy (ψ_{ph}): to calculate this factor, the values of enthalpy ($hi - hi_o$) and specific entropy ($si - si_o$) of each compound need to be available, but also the mass flow (y_i), at both operational and environmental temperature and pressure [44,47].

$$\psi_{ph} = y_i(hi - hi_o) - To(si - si_o) \tag{19}$$

- Chemical exergy (ψ_{ch}): it is associated with the starting chemical composition of a system from its chemical equilibrium state [35,44,47].

$$\psi_{ch} = \sum_i \left(y_i ex_{ch,i}\right) + ToR\sum_i y_i Ln(y_i) \tag{20}$$

where R is the ideal gas constant, and $ex_{ch,i}$ the specific chemical exergy of the compound.

- Exergy destruction ($\dot{Ex}_d$) : the difference that exists between the work that is potentially recoverable by the system (W) and effective work through reversible processes ($Wrev$) can be defined as exergy destruction [44,47,49,50]:

$$\dot{Ex}_d = W - Wrev = ToSgen \tag{21}$$

- Exergy efficiency: it is defined as the exergy destroyed due to the internal and external losses caused by irreversible processes [51]:

$$\eta_{ex} = \frac{\sum_{out} \dot{E}x_{out}}{\sum_{in} \dot{E}x_{in}} \tag{22}$$

The exergy analysis conducted on the process system of Stage I refers to several interconnected systems, according to the schematic sketched in Fig. 3: a mixing chamber to obtain the synthetic biogas and biomethane streams, a pump for water transport, the kettle to generate steam, the TR, in which the steam reforming reaction of biogas/biomethane is carried out, and last but not least the water vapor condenser, in which it is possible recovering heat.

In the Stage II, the exergy analysis deals with the membrane separation process (Fig. 1).

Table 3 shows the exergy rate balance equations of all components in the whole system under a controlled volume, which have been developed based on the careful exergy analysis developed in [45]. Some assumptions were made to carry out the exergy analysis:

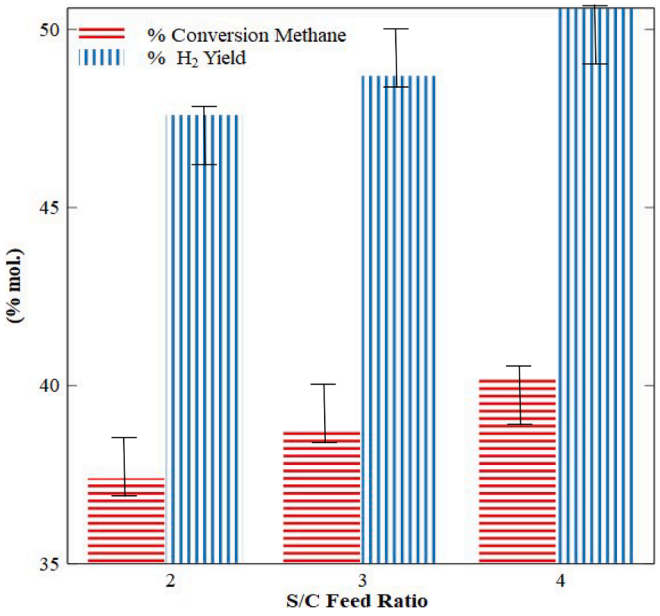

Fig. 3. Steam reforming of a synthetic biogas stream: methane conversion and H_2 yield vs S/C feed ratio at 873 K and 1 bar.

Table 3
The equations of equilibrium exergy rate of all components in the two stages system under a controlled volume.

Component	Exergy Balance
Mix-1	$\dot{E}x_1 + \dot{E}x_2 - \dot{E}x_3 + \dot{E}Q + \dot{E}W + \dot{E}x_d = 0$
Pump of Water	$\dot{E}x_4 - \dot{E}x_5 + \dot{E}Q + \dot{E}W_{pump} + \dot{E}x_d = 0$
Boiler	$\dot{E}x_5 - \dot{E}x_6 + \dot{E}Q_{boiler} - \dot{E}W + \dot{E}x_d = 0$
Mix-2	$\dot{E}x_6 + \dot{E}x_3 - \dot{E}x_7 + \dot{E}Q - \dot{E}W + \dot{E}x_d = 0$
Traditional Reformer	$\dot{E}x_7 - \dot{E}x_8 + \dot{E}Q_{reactor} + \dot{E}W + \dot{E}x_d = 0$
Condenser	$\dot{E}x_8 - \dot{E}x_9 - \dot{E}x_{10} - \dot{E}Q_{cond} + \dot{E}W + \dot{E}x_d = 0$
Membrane separator	$\dot{E}x_9 - \dot{E}x_{11} - \dot{E}x_{12} + \dot{E}Q_{MS} + \dot{E}W + \dot{E}x_d = 0$

- The pressure drop across the traditional reformer and membrane separator is assumed zero.
- The reforming process and membrane separation are kept at constant temperatures by an external heat supply.
- Dead state: the temperature (T_0) = 273.15 K and pressure (P_0) = 1 bar.
- Kinetic and potential exergies are negligible.
- The thermophysical properties of each species (water, methane, CO_2, CO, hydrogen, nitrogen) involved in the process such as specific enthalpy, specific entropy, specific flow exergy, etc. at set temperature and pressure are derived from thermodynamic and physical properties data extracted from [52].
- The specific chemical exergy is taken for each species from [46,53,54].

4. Results and discussion

4.1. Stage I: Steam reforming of synthetic biogas/biomethane

The experimental campaign started heating up the TR up to a temperature of 873 K, kept constant in the whole set of the reaction tests. At ambient pressure, the steam reforming of the synthetic biogas stream (Table 1) has been carried out, and the influence of S/C ratio has been analyzed. Fig. 3 shows the variation of methane conversion and hydrogen yield as a function of S/C ratio, evidencing that an increase of steam is responsible for a slight increment of conversion from 37 % at S/C = 2/1 to 40 % at S/C = 4/1. On the other hand, hydrogen yield is enhanced from 47 % at S/C = 2/1 to 52 % at S/C = 4/1. The modest improvement of conversion and hydrogen yield is mainly due to two effects: the presence of a reaction product such as CO_2 in the feed, which acted against the thermodynamic of methane steam reforming, and the limited operating temperature. Nevertheless, this temperature has been selected to limit the huge energy inputs required to carry out the reaction in the TR at higher temperatures (>873 K).

On the contrary, using the synthetic biomethane stream, the performance of the TR in terms of methane conversion and hydrogen yield resulted to be superior to those obtained using the synthetic biogas stream. In particular, methane conversion was improved from 50 % at S/C = 2/1 to 60 % at S/C = 4/1, while the hydrogen yield was enhanced from 45 % at S/C = 2/1 to 53 % at S/C = 4/1, Fig. 4. The better performance shown in the latter figure have been due to the lower presence of CO_2 in the feed, which did not affect significantly the thermodynamic of the methane steam reforming reaction, but also to the higher methane content in the biomethane stream, which involved a higher hydrogen production than the case of the biogas stream utilization.

In both cases, the carbon balance between the TR inlet and outlet streams evidenced no coke formation because it was closed with a maximum error lower than 2 %. Furthermore, feeding oxygen in the catalytic bed of the TR after each reaction test at a selected S/C feed ratio, the formation of CO_2 would have been expected in case of coke formed and deposited on the catalytic bed. Nevertheless, no CO_2 has been observed by GC, confirming further the absence of coke formation during the catalytic tests.

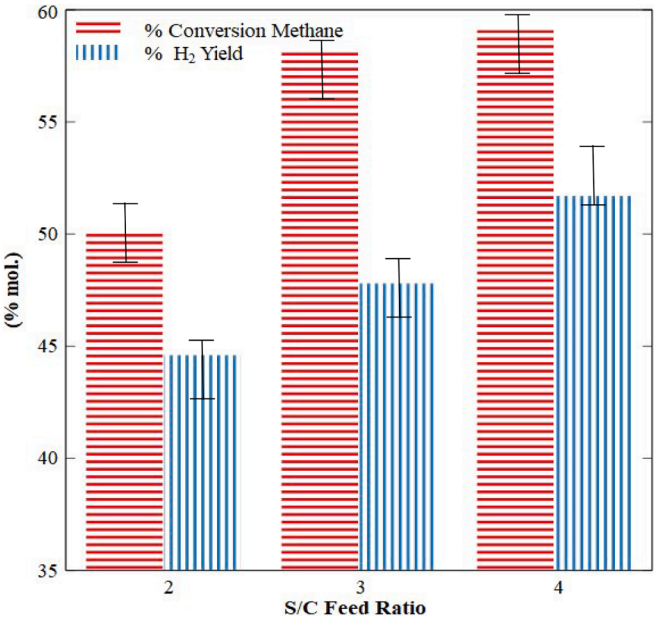

Fig. 4. Steam reforming of a synthetic biomethane stream: methane conversion and H_2 yield vs S/C feed ratio at 873 K and 1 bar.

It is also interesting to observe the products distribution in the reformed stream coming out from the TR at the different S/C feed ration studied in this work. Table 4 reports the molar fraction (dry basis) of the reformed stream in case of synthetic biogas utilization in the feed. As expected, the higher the S/C ratio the higher the hydrogen molar fraction in the reformed stream, whereas CO and CO_2 molar fractions exhibit oscillating values. It is worth of mentioning that this may happen when there is massive production of the desired product (hydrogen). Furthermore, a further reason may be found in the role of the reverse dry reforming of CO_2 reaction (4), which slows the consumption of CH_4 in the presence of high amounts of CO and hydrogen. Nevertheless, considering the progressive decrease of CH_4 molar fraction in the reformed stream, it is possible to affirm that the water gas shift (WGS) reaction (2) acted greatly. Therefore, the oscillation of CO_2 molar fraction value may be due to the combined influence of the reverse of DR and WGS reactions.

On the other hand, Table 5 shows the products distribution (dry basis) of the reformed stream in case of synthetic biomethane utilization in the feed. The reported values indicate that, although a slight decreasing trend of hydrogen molar fraction is noticeable when S/C feed ratio increases, both hydrogen yield and CH_4 conversion are increased. Hence, there is a contribution of another component, in the meantime produced with hydrogen. Table 5 confirms that this component is CO_2, whose concentration increases as S/C feed ratio rises. However, it is necessary to state that the production of hydrogen during the experimental phase was not slowed down, but only that this has been accompanied by other components production in the syngas stream coming out from the TR. In this case, CO_2 molar fraction increases monotonically and this may be attributable to the low weight of the DR reaction because methane is consumed during the SR reaction with steam. On the contrary, CO values oscillation may be due to the

Table 4
Reformed stream composition in the TR exercised at 873 K and 1 bar (biogas stream in the feed).

S/C[-]	x_{CH4} [% mol.]	x_{H2} [% mol.]	x_{CO2}[% mol.]	x_{CO} [% mol.]
2	11.4	40.7	25.1	22.9
3	9.8	44.7	22.5	23.0
4	9.2	47.2	30.9	12.8

Table 5
Reformed stream composition in the TR exercised at 873 K and 1 bar (biomethane stream in the feed).

S/C[-]	x_{CH4} [% mol.]	x_{H2} [% mol.]	x_{CO2}[% mol.]	x_{CO} [% mol.]
2	21.5	65.3	5.9	7.3
3	20.4	64.8	9.7	5.2
4	18.8	63.5	10.2	7.6

combined effect of the SR and WGS reactions: the former produces it, while the latter consumes it.

4.2. Stage II: Separation/purification of the H_2 rich-reformed stream

Prior to starting the experimental campaign foreseen in this study, the Pd-Ag membrane has been tested to single gas permeation tests to establish its hydrogen perm-selective performance. The tests have been realized using hydrogen and N_2 pure gases, varying the temperature from 673 K to 773 K and the total pressure between 1.5 (abs.) and 3.5 bar (abs). Fig. 5a shows the hydrogen flux permeating through the membrane as a function of the hydrogen permeation driving force across the membrane, which has been expressed in this case as the hydrogen partial pressure square root difference between the retentate and permeate sides. As illustrated in this figure, the hydrogenpermeating flux increases linearly with the hydrogen permeation driving force as confirmed by the linear regression factor (R^2) superior to 99 % at each temperature investigated in this work. Furthermore, only hydrogen permeates through the membrane, confirming its full hydrogen perm-selective behavior. According to the aforementioned results, it is possible to state that the hydrogen permeation through the Pd-Ag membrane follows the Sieverts-Fick law, in which the hydrogen permeation limiting step is represented by the atomic hydrogendiffusion through the membrane bulk (23).

$$J_{H_2} = Pe(p^{0.5}_{H2-retentate} - p^{0.5}_{H2-permeate}) \text{Sieverts} - \text{Fick law} \quad (23)$$

where J_{H2} represents the hydrogen flux permeating through the membranes, Pe is the hydrogen permeance (equal to the ratio between the hydrogen permeability, P_{H2}, and the Pd-Ag membrane thickness, L), $p_{H2\text{-}retentate}$ and $p_{H2\text{-}permeate}$ are the hydrogen partial pressures in the retentate and permeate sides, respectively.

Fig. 5b illustrates the hydrogen permeability (P_{H2}) variation as a function of the reverse of temperature, in which it is evident that the higher the temperature the higher the permeability, confirming that the hydrogen permeability may be described with an Arrhenius-like equation (24).

$$P_{H_2} = P_{H_2.0} exp^{\left(-\frac{E_A}{RT}\right)} \quad (24)$$

where $P_{H2,0}$ is the pre-exponential factor (calculated by the graphical assessment of the hydrogen permeability logarithm vs 1000/T of Fig. 7b), E_A the apparent activation energy, R the universal gas constant, and T the temperature.

Substituting Eq. (24) in Eq. (23), the flux of hydrogen permeating through the Pd-Ag membrane may be expressed also according to the Richardson equation (Eq. (25):

$$J_{H_2} = \frac{P_{H2.0} exp^{\left(-E_A/RT\right)}\left(P^{0.5}_{H2retentate} - P^{0.5}_{H2permeate}\right)}{L} \quad (25)$$

The separation/purification of the hydrogen-rich reformed stream coming out from the TR of Stage I has been performed in the MS operated at different temperatures, from 673 K (this minimum temperature has been set in order to limit the possible detrimental effect due to CO adsorption on the Pd-Ag membrane surface, particularly intensive below this temperature) to 773 K (maximum temperature limit set by the membrane producer, Johnson Matthey), and pressures, from 1.5 bar to 3.5 bar, keeping constant membrane area, syngas and sweep-gas flow rates, hence representing a specific case-study. In this regard, Fig. 6 shows the MS performance in terms of hydrogen recovery obtained at different MS temperatures and pressures during the separation/purification of the reformed stream coming out from the TR, obtained carrying out the steam reforming of the synthetic biogas stream. In this figure, the targets of hydrogen recovery expected by the Clean Hydrogen Alliance have been also reported in order to compare the performance obtained in the MS with respect to those expected by the EU Agency. As shown in this figure, the higher the pressure the higher the hydrogen recovery. Indeed, a higher pressure determines a higher hydrogen permeation driving force across the Pd-Ag membrane, allowing to remove more hydrogen from the retentate side toward the permeate side, globally enhancing the recovery. The improvement of hydrogen recovery is much more evident at higher temperature as it determines an increase of hydrogen permeability. Hence, at 723 K, the hydrogen recovery varied from 50 % at $\Delta p = 1$ bar to 72 % at $\Delta p = 1.8$ bar, but it was always lower than the 'target 2024 (80 %)', while it was overcome at 773 K and $\Delta p = 1.8$ bar, reaching the value of 88 %. Higher trans-membrane pressure did not determine significant improvement of the hydrogen recovery, achieving a plateau value.

Fig. 7 sketches the hydrogen recovery of the MS acting on the reformed stream coming out from the TR of Stage I, in which the steam reforming of synthetic biomethane is carried out. As observed in the former case, hydrogen recovery increases by rising both temperature

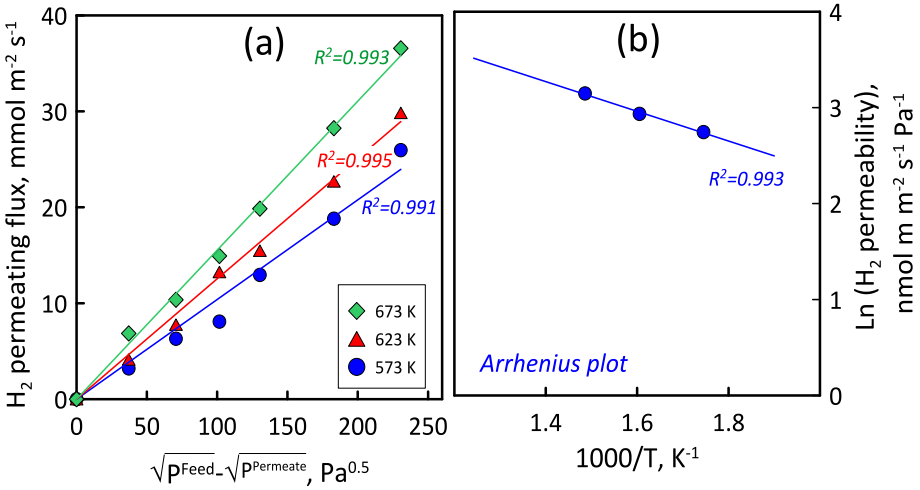

Fig. 5. A) h_2 permeating flux vs H_2 permeation driving force at different temperatures; b) H_2 permeability vs 1000/T.

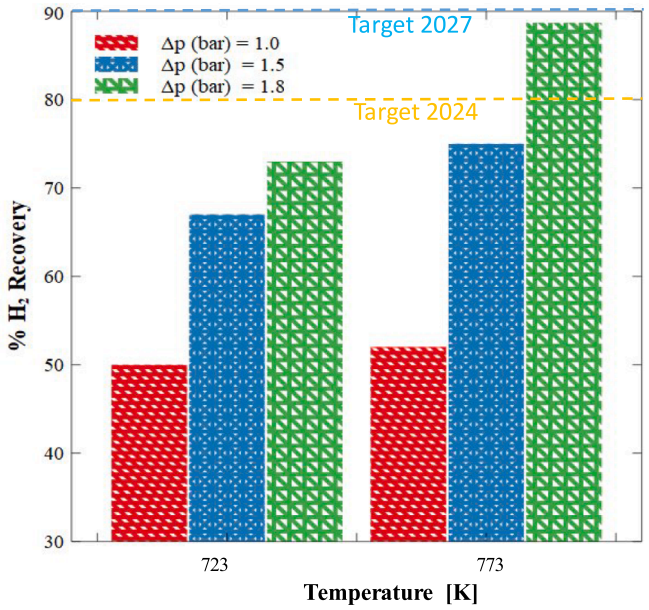

Fig. 6. Stage II – Pd-Ag membrane separator – H_2 separation/purification of the reformed stream coming out from the TR of Stage I (steam reforming of synthetic biogas): H_2 recovery at different temperatures and pressures compared to the EU Clean Hydrogen Alliance Targets.

and transmembrane pressure. In particular, according to Eq. (24) the higher the temperature the higher the hydrogen permeability, which allows that a higher quantity of hydrogen may permeate through the membrane, consequently enhancing the hydrogen recovery. On the other hand, the higher the pressure the higher the hydrogen partial pressure in the feed side, which is responsible for the consequent increase of the hydrogen partial pressure difference across the membrane (Eq. (23) and the H_2 permeability as well, globally contributing to improve the hydrogen recovery. Nevertheless, operating at 773 K and $\Delta p = 2.5$ bar, the MS has been able to overcome the 'hydrogen recovery target 2024′ set by the Clean Hydrogen Alliance and reach the 'target 2027′ equal to 90 %. No higher temperatures have been investigated due to the maximum allowed operating temperature (773 K) of the Pd-Ag membrane used in this work. Higher pressures have been not adopted because of the pressure limit imposed by the mechanical resistance of the membrane.

In the experimental data reported in Fig. 6,7, the deviations from the 'hydrogen recovery Target 2030′ were due to the relatively low hydrogen permeability of the Pd-Ag membrane caused by its tick metallic layer (150 μm), which was responsible for lower hydrogen recovery in the permeate side of the MS. On the other hand, the thick metallic layer of the Pd-Ag membrane allowed to reach a purity of the hydrogen recovered in the MS permeate side superior to 99.999 %, overcoming the 'hydrogen purity target 2030 (99.99 %)' set by the aforementioned EU Agency.

4.3. Energy efficiency and exergy analysis

The performance of the overall system (TR + MS) is mainly affected by temperature and pressure operating conditions.

The temperature is crucial during the processes since the chemical species involved in the chemical reactions inside the TR and the hydrogen flux passing through the membrane (MS) depend on it. Therefore, the overall energy efficiency of hydrogen production and separation is shown in Fig. 8 as a function of temperature and depending on the feed stream used in the first stage (biogas and biomethane). Energy efficiency is greatly improved when the process temperature is increased. Feeding biomethane to the TR, it is possible to observe a significant increase in energy efficiency from ~ 42 % at 673 K to ~ 72 % at 773 K, representing a substantial improvement. The same trend occurred feeding biogas to the TR, even though the improvement of the energy efficiency ranges from ~ 40 % at 723 K to 60 % at 773 K. The results show that the two stages process working with biomethane as feed stream involves higher thermal efficiency based on the lower heating value (LHV) than biogas, with a significant increase passing from 673 K to 773 K. This is demonstrated by considering the chemical composition and thermal properties of the species participating in the process. Since methane is the main component for producing hydrogen by steam reforming reaction, the higher methane concentration in the feed stream (biomethane) leads to a higher energy efficiency in the whole process of hydrogen production and separation. The increase of the thermal efficiency with the temperature can be explained in terms of

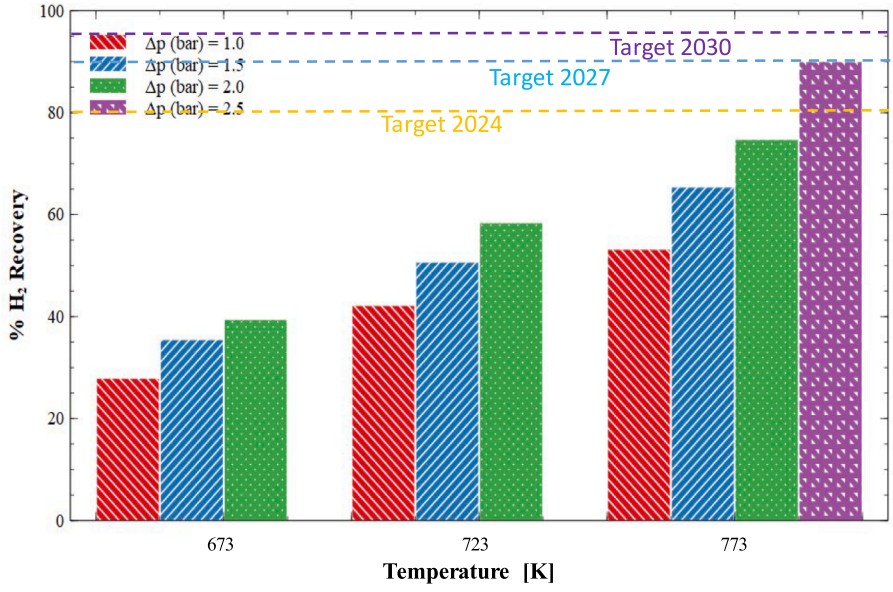

Fig. 7. Stage II – Pd-Ag membrane separator – H_2 separation/purification of the reformed stream coming out from the TR of Stage I (steam reforming of synthetic biomethane): H_2 recovery at different temperatures and pressures compared to the EU Clean Hydrogen Alliance Targets.

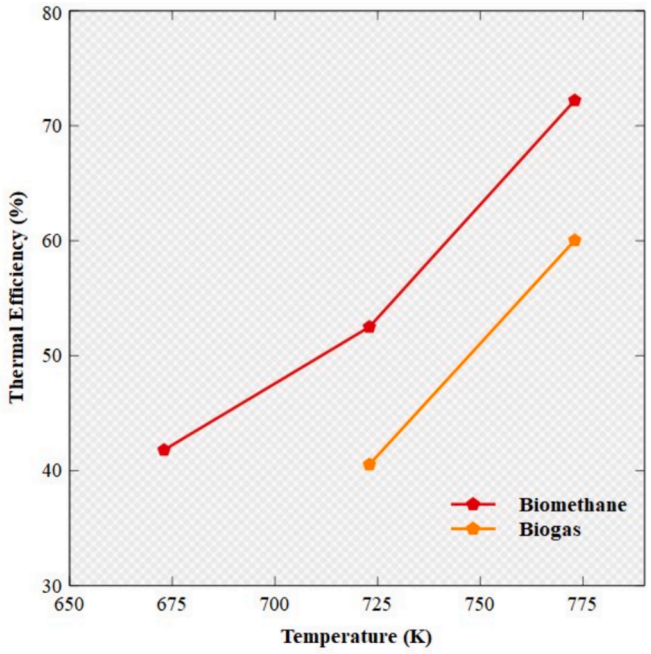

Fig. 8. Thermal efficiency based on LHV for biogas and biomethane.

the benefits due to an increase of temperature on the kinetics of the chemical reactions involved in the steam reforming process in the TR.

The various equations governing the overall process system are presented in Table 3, and the exergy analysis has been conducted following the procedure of thermodynamic analysis. Afterwards, the exergy fluxes have been determined for the specified control volumes, illustrating the exergy efficiency of the different processes carried out in Stage I and Stage II. Table 6 shows the derived values of the exergy analysis applied to each component of the overall system, distinguished into the steam reforming of biogas and biomethane in the TR of Stage I to take into account further the impact of the feed stream composition and process operating conditions on the overall exergy efficiency. In particular, exergy analysis has been based on this additional assumption regarding the mixing chamber. It enables the generation of synthetic biogas and biomethane streams, maintaining the following conditions: constant temperature and pressures, absence of chemical reactions within the chamber, and no interactions between the molecules. Consequently, during the process of the synthetic streams preparation, the exergy values of methane and carbon dioxide are transferred to the output stream of the system, resulting in no loss or reduction of the available work potential within the system.

The exergy analysis of the water pump for both processes yields practically identical values even though the water flow rate changes a bit as a consequence of the different CH_4 concentration of the two feeds. Regarding to the boiler, in order to respect the S/C ratio for the different CH_4 concentration of the biogas and biomethane streams, a higher exergy destruction ($2.2{\cdot}10^{-4}$ W) has been calculated for the biomethane stream, with a consequent lower exergy efficiency (90.4 %) than the case of biogas stream (91.2 %).

The exergy analysis applied to the TR in the Stage I, adopted to carry out the steam reforming of synthetic biogas, reveals an exergy destruction of 1.5 W, with an efficiency of 87.5 %. On the other hand, if synthetic biomethane steam reforming is carried out in the TR, the exergy destruction value is equal to 0.9 W and the exergy efficiency is 92.3 %. Comparing the two exergy analyses regarding the TR, it is evident that the utilization of biomethane (with higher methane content) is responsible for a relatively higher exergy efficiency compared to biogas. This indicates that the TR solution adopting biomethane as feed stream combined to steam experiences lower energy losses and allows higher system efficiency to be achieved.

The exergy analysis conducted at the condenser reveals an exergy destruction of 6.5 W, in case of biogas adoption, and 14.2 W in case of biomethane adoption. This is due to a higher amount of steam to be condensed in the case of biomethane stream adoption. Hence, higher values of exergy destruction may be attributed to the heat recovered from the process that can be taken back in the form of heat, useful for example in the water vaporization step. Consequently, the process efficiencies are determined to be for this device equal to 93.4 % in case of biogas steam reforming carried out in the TR and 94.8 % in case of biomethane steam reforming.

The exergy analysis applied to the hydrogen membrane separation step (Stage II) shows that its exergy destruction is equal to 0.5 W if the reformed stream coming out from Stage I is generated by steam reforming of biogas, whereas it is equal to 0.2 W if generated by steam reforming of biomethane. The analysis highlighted further that the hydrogen separation/purification at Stage II is more efficient (93.8 %) if its feed is constituted of a syngas coming from Stage I generated by steam reforming of biomethane, instead of a syngas generated by steam reforming of biogas (efficiency equal to 91.7 %). Indeed, according to Table 5, the reformed stream coming out from the TR (which represents the MS feed stream) is richer in hydrogen (around 64–65 %, varying the S/C ratio) if biomethane is used in the TR feed stream instead of biogas (hydrogen concentration between 41 and 47 % varying the S/C ratio, Table 4). This is the reason why the hydrogen permeation driving force across the membrane (based on the hydrogen partial pressure difference between feed and permeate side of the MS) is larger in the case of biomethane than biogas adoption, making, much more efficient the hydrogen separation. At 773 K, due to the larger hydrogen permeation driving force related to biomethane adoption in the TR feed stream, the MS was able to meet the 'standard 2027' of hydrogen recovery and purity ~~is realized~~ at higher transmembrane pressure (2.5 bar) than the ~~second~~ case of biogas adoption, in which the maximum transmembrane pressure ~~adopted~~ was equal to 1.8 bar. In particular, biomethane adoption in the TR feed stream is responsible for higher transmembrane pressure, which involves higher hydrogen permeation driving force, with a consequent increase of hydrogen permeation through the membrane, which reduces losses of available helpful energy and, consequently, the exergy destruction. On the other hand, using biogas, involves MS operations at lower hydrogen transmembrane partial pressure, which determines lower hydrogen permeation across the membrane and lower hydrogen recovery as well. Hence, to achieve the same MS performance in terms of hydrogen recovery obtained if biomethane is adopted in the TR feed stream, in the case of biogas adoption higher temperatures favoring higher hydrogen permeability through the Pd-Ag membrane (Eq. (23) are required, which necessarily involve higher energy consumption (exergy associated with heat to be supplied to the MS), consequently increasing the exergy destruction and

Table 6
Results of Exergy Destruction (EX_d) Analysis for the processes of Stage I and Stage II, distinguished into Biogas and Biomethane steam reforming carried out at 873 K and 1 bar.

Feed	Pump EX_d (W)	η_{ex}(%)	Boiler EX_d (W)	η_{ex}(%)	TR EX_d (W)	η_{ex}(%)	Condenser EX_d (W)	η_{ex}(%)	MS EX_d (W)	η_{ex}(%)
Biogas	$1.8{\cdot}10^{-5}$	91.7	$2.0{\cdot}10^{-4}$	91.2	1.5	87.5	6.5	93.4	0.5	91.7
Biomethane	$1.8{\cdot}10^{-5}$	91.7	$2.2{\cdot}10^{-4}$	90.4	0.9	92.3	14.2	94.8	0.2	93.8

decreasing the MS efficiency ($\eta_{ex} = 91.7$ % in case of biogas with respect to $\eta_{ex} = 93.8$ % in case of biomethane).

Fig. 9,10 show the distribution of exergy destruction among the main components of the process: traditional reformer, membrane separator, and condenser. The condensation stage shows the highest values of irreversibility, independently of the feed stream (biogas or biomethane) at the first stage (TR). However, we observed that, feeding biomethane to the TR, determines a higher irreversibility in the condensation stage being a purer current (rich in methane), then responsible for making the conversion process less challenging than the case in which biogas is fed to the TR, because it contains less methane. (SEE Fig. 10.).

To be a less demanding process, the syngas current coming out from the TR includes a certain amount of stored energy, since it is not fully used during the steam reforming process. Then, during the condensation phase, some of this energy is dissipated/lost, contributing to an increase in the irreversibility of the process. However, in both cases, the condensation process represents a significant source of irreversibility, which can be reduced through optimization and heat recovery techniques.

Feeding biomethane to the TR induces also lower irreversibility percentages in the TR and in the MS than in the case of biogas utilization as feed stream. Also in this case, it can be explained by the higher purity of biomethane that, during the reforming process, requires work, reducing the irreversibility of both TR and MS processes. In addition, the reformed stream is richer in hydrogen if the TR feeding stream is constituted of biomethane and, going to the MS, this higher percentage of hydrogen requires less energy to be separated and purified from the other by-products. However, according to Nalbant Atak et al. [45], the remaining irreversibility is due to the chemical reactions and kinetics of the reactions inside the TR.

Table 7 shows the overall exergy destructions of the overall system, which have been calculated by Eq. (22) for the two feeding mixture cases. In particular, the overall values have taken into account: a) $\dot{E}x_{in}$, which represents the input exergy values provided by biogas or biomethane stream (physical and chemical exergy of CH_4, CO, CO_2 and H_2) plus the steam exergy; b) $\dot{E}x_{out}$, which represents the output exergy of both MS permeate and retentate streams; c) $\dot{E}W_i$, which is the exergy associated to the work; and d) $\dot{E}Q_i$, which is the exergy associated to the heat supplied to the overall system (steam reformer + membrane separator) minus the heat recovered from the condenser.

In particular, it is possible to observe that the overall exergy destruction is equal to 92 % and 88 % in case biomethane or biogas are fed to the first stage of the overall system, respectively.

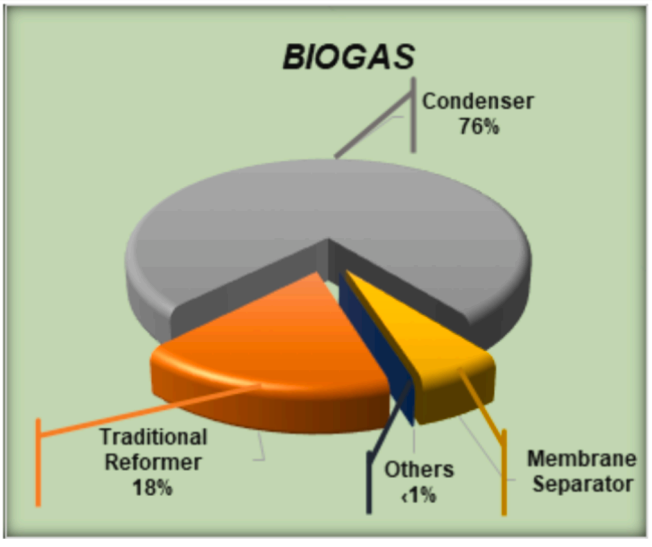

Fig. 9. Global values of exergy destruction rate (W) of each component according to the operating temperature of the integrate systems for biogas.

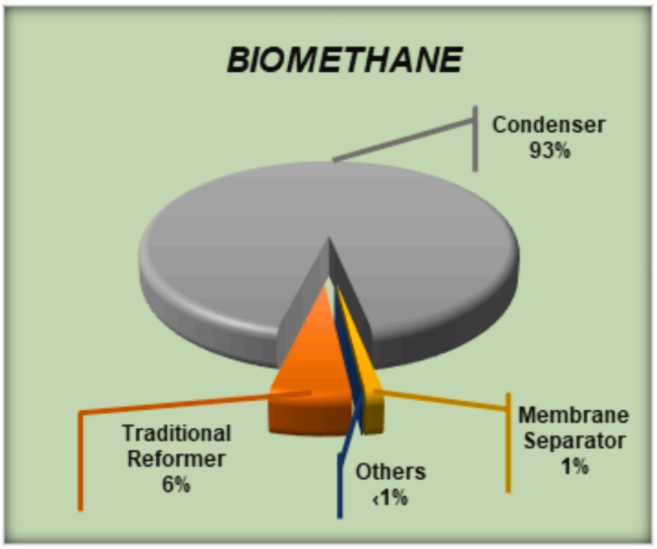

Fig. 10. Global values of exergy destruction rate (W) of each component according to the operating temperature of the integrate systems for biogas.

5. Conclusion

This work showed the effectiveness of the steam reforming process combined to a membrane separation stage to generate decarbonized hydrogen from biogas and/or biomethane, meeting the targets of the European Clean Hydrogen Alliance, further investigating the thermal efficiency and exergy destruction of the two stages system.

As a specific case-study realized keeping constant the space velocity and reaction temperature of the TR (first stage) as well as the membrane area, syngas and sweep-gas flow rates of the MS (second stage), the first stage, constituted of a TR used to carry out the steam reforming process, showed a maximum conversion of methane equal to 60 % and hydrogen yield equal to 53 % at 873 K, 1 bar and S/C = 4/1, using biomethane as feed stream, whereas 40 % of methane conversion and 52 % of hydrogen yield were reached at the same conditions, adopting biogas as feed stream. In the second stage process, the Pd-Ag membrane separator allowed to meet the 'decarbonized hydrogen targets 2027' set by the Clean Hydrogen Alliance agency, purifying the reformed stream coming out from the TR at 773 K and $\Delta p = 2.5$ bar, reaching a hydrogen recovery equal to 90 % with a purity of 99.9999 %, if biomethane was used as feed stream. Otherwise, the MS allowed only to overcome the 'decarbonized hydrogen targets 2024', with a hydrogen recovery equal to 88 % and a purity equal to 99.9999 %, in case biogas was used as feed stream at the first stage of the whole system.

Another important contribution obtained in this work was related to the exergy analysis carried out on the two stages system, investigating the impact of the feed stream composition and process operating conditions on the overall exergy efficiency. The exergy analysis highlighted that, feeding biomethane at the first stage, induces lower irreversibility percentages in the TR and in the MS than feeding biogas. This happened because the higher methane concentration in the biomethane stream required work during the reforming process, reducing the irreversibility at both TR and MS stages. As a consequence of the biomethane feed stream adoption, the reformed stream was richer in hydrogen and its higher percentage involved less energy in the MS to realize its high grade separation/purification from the other by-products. Furthermore, independently of the feed stream composition, the condensation stage represented the most significant source of irreversibility of the overall system (93 % of irreversibility in case of biomethane adoption, 73 % in case of biogas adoption), to be reduced necessarily by means of an

Table 7
Global values of exergy destruction (%) of the overall systems for biogas and biomethane.

Whole system	$\dot{E}x_{in}(W)$	$\dot{E}x_{out}(W)$	$\dot{E}W_i(W)$	$\dot{E}Q_i(W)$	$\dot{E}x_d(W)$	$\eta_{global\_Ex}(\%)$
Biogas	1.102	0.59	–	0.38	0.132	88
Biomethane	1.722	1.30	–	0.28	0.142	92

optimization and the heat recovery technologies in future studies. Last but not least, further results of this work showed that the overall system adopting biomethane as feed stream involves higher thermal efficiency, based on the LHV, than the adoption of biogas, as well as higher global values of exergy destruction, reaching the maximum value of around 72 % and 92 % (at 773 K), respectively.

The energy efficiency and exergy analyses carried out on the two stages system reported in this work constituted an important contribution useful to orientate future efforts in its technological development, encouraging further solutions for producing clean and sustainable hydrogen, thus contributing to the reduction of the greenhouse gas emissions. As a perspective of this study, considering that most of the irreversibilities present in the two stages system comes from the condensation stage, further studies should be oriented to the thermal optimization, particularly of the TR, trying to develop highly active catalysts to improve the steam reforming performance working at stoichiometric condition in order to avoid larger amount of unconverted and excess of water to be condensed. A further development of this work could be constituted of a much more intensified solution, such as a membrane reactor, in which the steam reforming of biogas/biomethane may be carried out at lower temperature (below 500 °C) than the conventional reformers, exploiting the membrane reactor advantages dealing with the simultaneous H_2 production and separation/purification realized in only one device, both in terms of better performance (higher methane conversion and H_2 yield than an equivalent TR) and energy efficiency (lower energy input due to lower MR operating temperatures), and operating, at least, under stoichiometric conditions (or under defect of steam) to reduce the irreversibilities due to the condensation stage.

CRediT authorship contribution statement

Henry Bryan Trujillo Ruales: . **Alex Spadafora:** Methodology, Investigation. **Piergiuseppe Fiore:** Investigation, Formal analysis, Conceptualization. **Jan Veres:** Visualization, Investigation. **Alessio Caravella:** Visualization. **Adolfo Iulianelli:** Writing – review & editing, Supervision, Project administration, Investigation, Funding acquisition, Formal analysis, Data curation, Conceptualization.

Declaration of competing interest

The authors declare that they have no known competing financial interests or personal relationships that could have appeared to influence the work reported in this paper.

Data availability

Data will be made available on request.

Acknowledgements

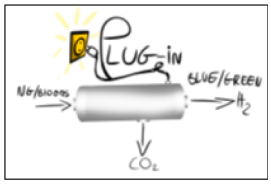

"PLUG-IN - Process for Low-carbon blUe & green hydrogen Generation via Intensified electrified reforming of Natural gas/biogas" project (PRIN_Bando MUR 2020, Prot. 2020N38E75, D.D. 2436 del 20/10/2021), and the European Union – NextGeneration EU from the Italian Ministry of Environment and Energy Security POR H2 AdP MMES/ENEA with involvement of CNR and RSE, PNRR - Mission 2, Component 2, Investment 3.5 "Ricerca e sviluppo sull'idrogeno", are acknowledged to support this work

References

[1] Liu Z-F, Zhao S-X, Zhao S-L, You G-D, Hou X-X, Yu J-L, et al. Improving the economic and environmental benefits of the energy system: A novel hybrid economic emission dispatch considering clean energy power uncertainty. Energy 2023;285:128668.
[2] Khan I, Zakari A, Zhang J, Dagar V, Singh S. A study of trilemma energy balance, clean energy transitions, and economic expansion in the midst of environmental sustainability: New insights from three trilemma leadership. Energy 2022;248:123619.
[3] UNFCCC, "Paris Agreement" Conf. Parties its twenty-first Sess,"*55 Int'l Legal Materials 743 (2016)*, p. 32, 2015.
[4] Dincer I. Covid-19 coronavirus: Closing carbon age, but opening hydrogen age. International Journal of Energy Research 2020;44:6093–7.
[5] Bi Y, Ju Y. Design and analysis of an efficient hydrogen liquefaction process based on helium reverse Brayton cycle integrating with steam methane reforming and liquefied natural gas cold energy utilization. Energy 2022;252:124047.
[6] Calik E, Ates EB. Developing an assessment scale for public awareness of hydrogen energy. Sustain Energy Techn Assessm 2023;56:103057.
[7] Dincer I. Hydrogen 1.0: A new age. *Int J Hydrogen Energy* 2023;43:16143–7.
[8] Balat M. Potential importance of hydrogen as a future solution to environmental and transportation problems. International Journal of Hydrogen Energy 2008;33:4013–29.
[9] Hren R, Vujanović A, Van Fan Y, Klemeš JJ, Krajnc D, Čuček L. Hydrogen production, storage and transport for renewable energy and chemicals: An environmental footprint assessment. Renewable and Sustainable Energy Reviews 2023;173:113113.
[10] Gupta P, Kurien C, Mittal M. Biogas (a promising bioenergy source): A critical review on the potential of biogas as a sustainable energy source for gaseous fuelled spark ignition engines. International Journal of Hydrogen Energy 2023;48:7747–69.
[11] Huang J, Feng H, Huang L, Ying X, Shen D, Chen T, et al. Continuous hydrogen production from food waste by anaerobic digestion (AD) coupled single-chamber microbial electrolysis cell (MEC) under negative pressure. Waste Managem 2020;103:61–6.
[12] Park MJ, Kim JH, Lee YH, Kim HM, Jeong DW. System optimization for effective hydrogen production via anaerobic digestion and biogas steam reforming. International Journal of Hydrogen Energy 2020;45:30188–200.
[13] Ugarte P, Durán P, Lasobras J, Soler J, Menéndez M, Herguido J. Dry reforming of biogas in fluidized bed: Process intensification. International Journal of Hydrogen Energy 2017;42:13589–97.
[14] Di Marcoberardino G, Foresti S, Binotti M, Manzolini G. Potentiality of a biogas membrane reformer for decentralized hydrogen production. Chem Eng Proc - Process Intens 2018;29:131–41.
[15] Voitic G, Pichler B, Basile A, Iulianelli A, Malli K, Bock S, et al. In: 10 in Fuel Cells and Hydrogen: From Fundamentals to Applied Research. Amsterdam: Elsevier B.V; 2018. p. 215–41. https://doi.org/10.1016/B978-0-12-811459-9.00010-4. ISBN 9780128114599,.
[16] Sircar S, Golden TC. Purification of Hydrogen by Pressure Swing Adsorption, *Separ.* Science and Technology 2000;35:667–87.
[17] Oh H, Kalidindi SB, Um Y, Bureekaew S, Schmid R, Fischer RA, et al. A cryogenically flexible covalent organic framework for efficient hydrogen isotope separation by quantum sieving. Angewandte Chemie Int Ed 2013;52:13219–22.
[18] Liu C, Zhang X, Zhai J, Li X, Guo X, He G. Research progress and prospects on hydrogen separation membranes. Clean Energy 2023;7:217–41.
[19] Iulianelli A, Drioli E. Membrane engineering: latest advancements in gas separation and pre-treatment processes, petrochemical industry and refinery, and future perspectives in emerging applications. Fuel Proc Techn 2020;206:106464–97.

[20] Pal N, Agarwal M, Maheshwari K, Solanki YS. A review on types, fabrication and support material of hydrogen separation membrane. Materials Today: Proceedings 2020;28:1386–91.

[21] Shiraz HG, Shiraz MG. Palladium nanoparticle and decorated carbon nanotube for electrochemical hydrogen storage. International Journal of Hydrogen Energy 2017; 42:11528–33.

[22] Weber M, Drobek M, Rebière B, Charmette C, Cartier J, Julbe A, et al. Hydrogen selective palladium-alumina composite membranes prepared by Atomic Layer Deposition. J Membrane Sci 2020;596:117701.

[23] Goh PS, Ismail AF, Sanip SM, Ng BC, Aziz M. Recent advances of inorganic fillers in mixed matrix membrane for gas separation. Sep Purif Techn 2011;81:243–64.

[24] Cardoso SP, Azenha IS, Lin Z, Portugal I, Rodrigues AE, Silva CM. Inorganic Membranes for Hydrogen Separation. Separation and Purification Reviews 2018; 47:229–66.

[25] Balachandran U, Lee T, Chen L, Song S, Picciolo J, Dorris S. Hydrogen separation by dense cermet membranes. Fuel 2006;85:150–5.

[26] A. Basile, A. Gugliuzza, A. Iulianelli, P. Morrone, Membrane technology for carbon dioxide (CO_2) capture in power plants, Ch. 5 in Advanced membrane science and technology for sustainable energy and environmental applications, ed. A. Basile and S.P. Nunes, Woodhead publishing Series in Energy – Cornwall (UK), 2011, ISBN: 978184569969-7, pp.113-159.

[27] Caro J, Noack M, Kölsch P, Schäfer R. Zeolite membranes – state of their development and perspective. Microp Mesop Mater 2000;38:3–24.

[28] Iulianelli A, Ghasemzadeh K, Marelli M, Evangelisti C. A supported Pd-Cu/Al_2O_3 membrane from solvated metal atoms for hydrogen separation/purification. Fuel Proc Techn 2019;195:106141–9.

[29] A. Iulianelli, M. Manisco, A. Figoli, K. Ghasemzadeh, Dense metal membranes for syngas purification, Ch. 12 In Advances in Synthesis Gas: Methods, Technologies and Applications: Syngas Purification and Separation, (M.R. Rahimpour, M.A. Makarem, M. Meshksar Eds.), Elsevier, ISBN: 9780323918770,1st of November (2023), pp. 325-340. https://doi.org/10.1016/B978-0-323-91877-0.00008-8.

[30] Alique D, Martinez-Diaz D, Sanz R, Calles JA. Review of supported Pd-based membranes preparation by electroless plating for ultra-pure hydrogen production. Membranes 2018;8:5.

[31] Ghasemzadeh K, Morrone P, Iulianelli A, Liguori S, Babaluo AA, Basile A. H_2 production in silica membrane reactor via methanol steam reforming: modeling and HAZOP analysis. International Journal of Hydrogen Energy 2013;38: 10315–26.

[32] Razmjoo A, Shirmohammadi R, Davarpanah A, Pourfayaz F, Aslani A. Stand-alone hybrid energy systems for remote area power generation. Energy Reports 2019;5: 231–41.

[33] Mehdizadeh-Fard M, Pourfayaz F, Maleki A. Exergy analysis of multiple heat exchanger networks: An approach based on the irreversibility distribution ratio. Energy Reports 2021;7:174–93.

[34] Murmura MA, Vilardi G. Energy and exergy analysis of the zinc/zinc oxide thermochemical cycle for hydrogen production and fuel cell power generation. Energy Conv Managm 2021;247:114761.

[35] Ofori-Boateng C, Lee KT. Comparative thermodynamic sustainability assessment of lignocellulosic pretreatment methods for bioethanol production via exergy analysis. Chemical Engineering Journal 2013;228:162–71.

[36] Xiong Q, Vaseghi M, Ali JA, Tlili I, Li Z. Nanoparticle application for heat transfer and irreversibility analysis in an air conditioning unit. J Molec Liquids 2019;292: 111372.

[37] Dehdashtijahromi M, Binazadeh M, Farsi M. Dynamic modeling, optimization and exergy analysis of novel membrane reactor for enhanced olefin and pure hydrogen production via heavy paraffin dehydrogenation. International Journal of Hydrogen Energy 2024;51:225–42.

[38] Clean Hydrogen Partnership, Strategic Research and innovation Agenda 2021-2027. https://www.clean-hydrogen.europa.eu/about-us/key-documents/strategicresearch-and-innovation-agenda_en, Accessed January 2024.

[39] A. Hedayati, O. Corre, B. Lacarrière, J. Llorca, Exergy and energy evaluation of bio-ethanol steam reforming in a catalytic membrane reactor, Conference: 7th International Exergy, Energy and Environment Symposium - IEEES-7At: Valenciennes, France, Volume: 7, 2015.

[40] Nalbant Atak Y, Colpan CO, Iulianelli A. Energy and exergy analyses of an integrated membrane reactor + CO_2 capture system to generate decarbonized hydrogen. Energy Conv Managm 2022;272:116367.

[41] Nafees T, Bhatti AA, Jadoon UK, Ahmad F, Ahmad I, Kano M, et al. Model-based quality, exergy, and economic analysis of fluidized bed membrane reactors. Membranes 2021;11:765.

[42] Mokhatab S, Poe WA, Mak JY. Energy and Exergy Analyses of Natural Gas Processing Plants, in *Handbook of Natural Gas Transmission and Processing*. Elsevier 2019:669–739. https://doi.org/10.1016/b978-0-12-815817-3.00022-8.

[43] Italiano C, Drago Ferrante G, Pino L, Laganà M, Ferraro M, Antonucci V, et al. Silicon carbide and alumina open-cell foams activated by Ni/CeO_2-ZrO_2 catalyst for CO_2 methanation in a heat-exchanger reactor. Chemical Engineering Journal 2022;434:134685.

[44] Bejan A. Fundamentals of exergy analysis, entropy generation minimization, and the generation of flow architecture. International Journal of Energy Research 2002; 26:1–43.

[45] E. Querol, B. Gonzalez-Regueral, J.L. Perez-Benedito, Practical approach to exergy and thermoeconomic analyses of industrial processes, London: Springer., ISBN 978-1-4471-4621-6, 2012, pp. 1-84.

[46] Abuşoğlu A, Özahi E, Kutlar Aİ, Demir S. Exergy analyses of green hydrogen production methods from biogas-based electricity and sewage sludge. International Journal of Hydrogen Energy 2017;42:10986–96.

[47] Obodeh O. Time-Dependent Exergy Analysis of a 120 MW Steam Turbine Unit of Sapele Power Plant. American J Electric Power Energy Syst 2013;2:129.

[48] T.J. Kotas, The exergy method of thermal plant analysis, Paragon Publishing, ISBN 978-1908341891, 2012, pp. 1-352.

[49] Zhang F, Zhu L, Rao D. The evaluation of a methane autothermal chemical looping reforming experiment based on exergy analysis. RSC Advances 2019;9:22032–44.

[50] Chouhan K, Sinha S, Kumar S, Kumar S. Utilization of biogas from different substrates for SOFC feed via steam reforming: Thermodynamic and exergy analyses. J Environm Chem Eng 2019;7:103018.

[51] van der Ham LV, Kjelstrup S. Exergy analysis of two cryogenic air separation processes. Energy 2010;35:4731–9.

[52] C.L. Yaws, Handbook of Chemical Compound Data for Process Safety - Comprehensive Safety and Health-Related Data for Hydrocarbons and Organic Chemicals Selected Data for Inorganic Chemicals, Gulf Professional Publishing, ISBN: 978-0-88415-381-8, 1997, pp. 1-226.

[53] Gharagheizi F, Ilani-Kashkouli P, Hedden RC. Standard molar chemical exergy: A new accurate model. Energy 2018;158:924–35.

[54] Xiang JY, Cali M, Santarelli M. Calculation for physical and chemical exergy of flows in systems elaborating mixed-phase flows and a case study in an IRSOFC plant. International Journal of Energy Research 2004;28:101–15.